Mode Demultiplexers for Rectangular Multimode Waveguides

Junhe Zhou, *Member, IEEE*, and Philippe Gallion, *Senior Member, IEEE*

***Abstract*— In this letter, the mode demultiplexers for rectangular multimode waveguides are proposed based on a spatial sampling and the multimode interference (MMI) effect. The modes of the rectangular waveguide are sampled by an equally spaced waveguide array and become the supermodes of the array. The supermodes are passed to a MMI coupler with phase shifters at the input ports. Owing to the MMI effect, the output optical field will concentrate on the corresponding output port, whose port number coincides with the order of the mode inside the rectangular waveguide.**

***Index Terms*— Multimode waveguides, mode division multiplexing.**

I. Introduction

MODE division multiplexing (MDM) has been considered as a promising technique to further increase the capacity of the optical fiber communication system [1]. The bottleneck to implement this technique is to realize key components like mode multiplexers/de-multiplexers (MUXs/DEMUXs). The traditional free space multiplexing techniques [2], [3] are mature, but they have quite a complex structure and are difficult to be integrated into the fiber system.

Rectangular waveguides, including planar multimode waveguides and rectangular core fibers, are used in various applications, including the MDM systems. In particular, like circular core fibers, rectangular core fibers are easy to fabricate [4] and support multimode transmission [5]. In this letter, we propose to discriminate the modes of rectangular multimode waveguides by a sampling waveguide array and a multimode interference (MMI) coupler with phase shifters. MMI couplers [6]–[9] have been used as mode generators and mode converters [10]–[13] for planar multimode waveguides and mode MUXs/DEMUXs for multi-core waveguides [14], [15]. The device proposed here uses the structure in [14] and [15] along with a mode sampling waveguide array, which samples the mode profiles of rectangular waveguides and transforms them into the super-modes of the array. By exploiting the close relationship between the modes of the rectangular waveguides and the super-modes of the multi-core waveguides and implement the MUXs-DEMUXs proposed in [14] and [15], the modes of the rectangular waveguides are de-multiplexed.

In comparison with other mode MUXs/DEMUXs, the proposed device is fiber based and easier to be integrated into the fiber system. More importantly, the number of the modes to be de-multiplexed can be easily increased without significant modification of the device structure. It is worth mentioning that the relationship between the modes in rectangular waveguides with the super-modes of the waveguide array might be extended to the case of the cylindrical waveguides (traditional multimode fibers), which is of great significance in MDM systems.

II. Mathematical Description

A. Discrete Sampling of the Mode Inside the Multimode Waveguide

Without loss of generality, the rectangular waveguide is assumed to have its width much larger than its height and is considered as single mode in the y direction and multimode in the x direction [4]. As indicated in [4], such rectangular waveguides are commonly used and are easy to fabricate via the fiber technology. For such a waveguide, its modal analysis can be simplified as a one-dimensional (1D) waveguide modal problem. It should be noted that the method discussed here can be easily extended to the case of multimode rectangular waveguides which are multimode both in the x direction and the y direction. This can be done by using the two-dimensional (2D) MMI effect. Similarly to the 1D case, the DEMUX can be realized by a 2D sampling waveguide array followed by a 2DMMI coupler with phase shifters [15].

The modes inside the 1D multimode waveguide is [6]–[9]

$$E_m = \sin\left(\frac{m\pi x}{W_e}\right) \quad (1)$$

where m is the mode number, W_{e} the effective width of the multimode waveguide. $N-1$ equally spaced waveguides are used to sample the mode field and the sampling process takes place at

$$x_i = \frac{iW_e}{N} \quad (i = 1 \cdots N-1) \quad (2)$$

The effective widths of the sampling waveguides are w, and those waveguides are single mode. The mode profile of

Manuscript received September 20, 2014; revised November 16, 2014; accepted November 21, 2014. Date of publication December 4, 2014; date of current version January 21, 2015. This work was supported by the National Science Foundation of China under Grant 61201068.

J. Zhou is with the Department of Electronics Science and Engineering, Tongji University, Shanghai 200092, China (e-mail: jhzhou@tongji.edu.cn).

P. Gallion is with the Laboratory for Communication and Processing of Information, Centre National de la Recherche Scientifique, École Nationale Supérieure des Télécommunications, TELECOM ParisTech, Paris 75013, France (e-mail: philippe.gallion@telecom-paristech.fr).

Color versions of one or more of the figures in this letter are available online at http://ieeexplore.ieee.org.

Digital Object Identifier 10.1109/LPT.2014.2375208

the i^{th} waveguide is approximately

$$f_i(x) = \begin{cases} \sin\left(\frac{\pi\left(x - x_i + \frac{w}{2}\right)}{w}\right) & -\frac{w}{2} + x_i < x < \frac{w}{2} + x_i \\ 0 & else\ where \end{cases} \quad (3)$$

If mode m is sampled by those waveguides, the amplitudes of the fields within the sampling waveguides can be calculated by computing the overlap integral of Eq. (1) and Eq. (3)

$$\begin{aligned} a_i &= \int_{x_i - \frac{w}{2}}^{x_i + \frac{w}{2}} \sin\left(\frac{m\pi x}{W}\right) \sin\left(\frac{\pi\left(x - x_i + \frac{w}{2}\right)}{w}\right) dx \\ &= \cos\left(\frac{m\pi w}{2W}\right) \left(\frac{\frac{2\pi}{w}}{\left(\left(\frac{\pi}{w}\right)^2 - \left(\frac{m\pi}{W}\right)^2\right)}\right) \sin\left(\frac{mi\pi}{N}\right) \quad (4) \end{aligned}$$

When w approaches 0, a_i can be approximated by

$$\hat{a}_i \approx \sin\left(\frac{mi\pi}{N}\right) \frac{2w}{\pi}. \quad (5)$$

B. Super-Modes of the Waveguide Array

According to [16], a waveguide array with $N-1$ equally spaced waveguides has $N-1$ sinusoidal super-modes. The m^{th} super-mode of the i^{th} waveguide has the amplitude as [16]

$$\sin\left(\frac{mi\pi}{N}\right) \quad (6)$$

Comparing with the coefficients in Eq. (4-5), surprising coincidence occurs if the constants are ignored. Therefore, if the m^{th} mode of the rectangular waveguide is sampled by the array, it becomes the m^{th} super-mode of the array.

It should be noted that although the above relationship between the sampled mode field and the super-mode of the waveguide array has been derived based on the 1D waveguide modal analysis, it is valid when the y directional modal distribution is single mode and can be extended to the 2D case.

C. Mode Discrimination

As indicated by [14], the super-modes of the 1D waveguide array can be discriminated by a 1DMMI coupler with phase shifters at the input ports. One can refer to [14] for details. For readers' conveniences, it is briefly expressed as follows.

The length of the MMI coupler should fulfill [6], [7], [14]

$$L_N = \frac{2nW_e^2}{N\lambda_0} \quad (7)$$

where n_{eff} is the effective index of the fundamental mode of the MMI coupler, λ_0 the free space wavelength, W_e the effective width/height of the MMI coupler, which is equal to the effective width of the rectangular waveguide. The input and output ports are located at the positions according to Eq. (2).

If the phase shifter array has the phase shift of $\frac{i^2\pi}{2N}$ and is placed at the input ports, the input and the output are related to each other via matrix **M**, with its elements as [6], [7], and [14]

$$M(l,k) = j\exp\left(j\frac{\pi}{4}\right)\sqrt{\frac{2}{N}}\exp\left(-j\frac{l^2\pi}{2N}\right)\sin\left(\frac{lk\pi}{N}\right) \quad (8)$$

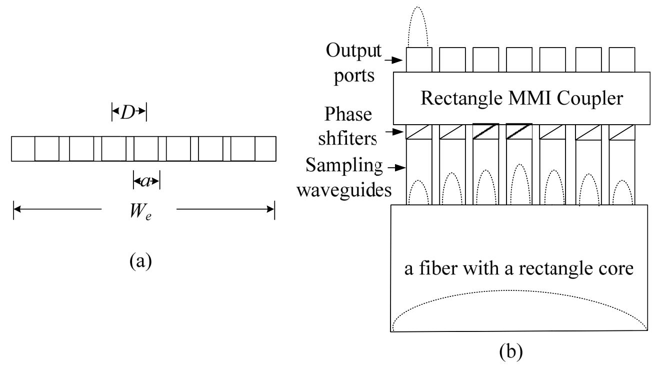

Fig. 1. Schematic of the device (a) the cross section of the device, (b) the top view of the device and the illustration of the modal profiles.

Comparing Eq. (6) with Eq. (8), it can be observed that the rows of the matrix **M** are the same as the vectors in Eq. (6) despite some constant coefficients. Therefore, if a super-mode of the waveguide array is injected into the input ports of the MMI coupler, the output optical intensity will concentrate at one output port whose port number matches the super-mode order. Therefore, if the m^{th} mode of the rectangular waveguide is sampled, it becomes the m^{th} super-mode of the waveguide array, and the MMI coupler based device can distinguish it at port m.

III. Numerical Results and Discussion

To verify the functionality of the proposed device, numerical simulations have been carried out on a rectangular fiber and its mode DEMUX by using the three dimensional beam propagation method (3DBPM). The materials for the fiber and the DEMUX are similar to those of [17]. For readers' convenience, it is restated here. The cladding has a refractive index of 1.45 and the core has a higher refractive index of 1.4674. Such a small index difference makes the polarization effect negligible. The rectangular core fiber has the effective width of 56μm and the height of 5μm. The sampling waveguides are assumed to be single mode rectangular waveguides. They have an equal core spacing of 8μm. It should be noted that the sampling waveguides can also be circular waveguides. The MMI device is a piece of rectangular core fiber, whose width and height are exactly the same as the previous one. The sampling waveguides and the MMI coupler have the same core and cladding refractive indexes as the rectangular core fiber. The signal wavelength is 1550nm and the MMI coupler length is determined by Eq. (7) and is slightly adjusted to 752μm. Phase shifters can be either realized by bending array waveguides or MCFs with different refractive indexes at different cores [17]. In this simulation, external phase shifters are placed between the sampling waveguides and the MMI device [18], which provide perfect phase shift without affecting the phase of other cores. The schematic of the device is in Fig. 1.

To demonstrate mode de-multiplexing capability, different modes of the rectangular core fiber are passed onto the sampling waveguides. The original modes (mode 1, 2, 6, 7) of the rectangular core fiber are plotted in Fig 2(a)–Fig 5(a). The widths of sampling waveguides are assumed to be

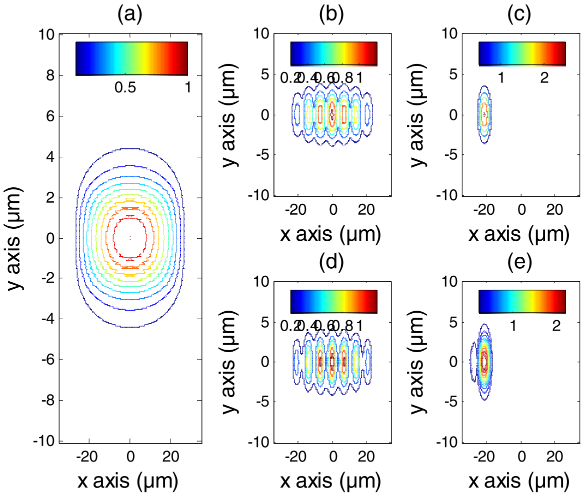

Fig. 2. The field at DEMUX input and output when the 1st mode of the rectangular core fiber is injected. (a) 1st mode of the rectangular core fiber; (b) the field sampled by the waveguide array with the width of 5μm; (c) output field of the DEMUX when the sampling waveguide is 5μm in width; (d) the field sampled by the waveguide array with the width of 3μm; (e) output field of the DEMUX when the sampling waveguide is 3μm in width.

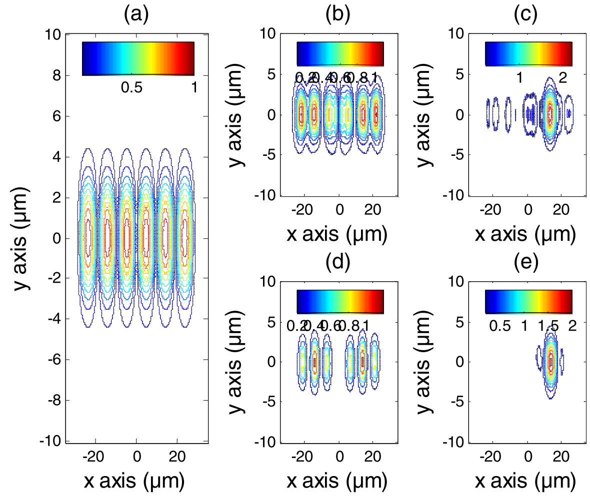

Fig. 4. The field at DEMUX input and output when the 6th mode of the rectangular core fiber is injected. (a) 6th mode of the rectangular core fiber; (b) the field sampled by the waveguide array with the width of 5μm; (c) output field of the DEMUX when the sampling waveguide is 5μm in width; (d) the field sampled by the waveguide array with the width of 3μm; (e) output field of the DEMUX when the sampling waveguide is 3μm in width.

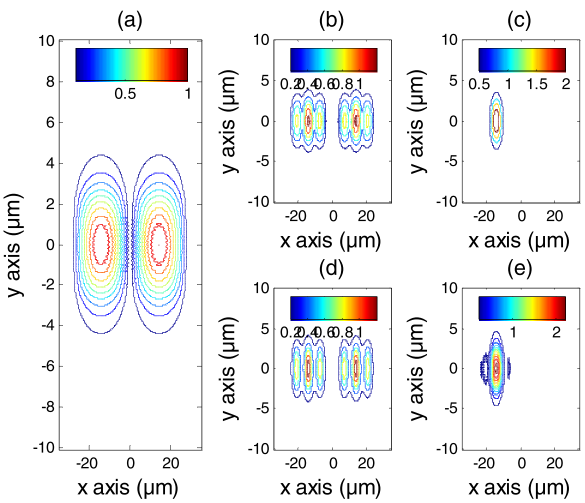

Fig. 3. The field at DEMUX input and output when the 2nd mode of the rectangular core fiber is injected. (a) 2nd mode of the rectangular core fiber; (b) the field sampled by the waveguide array with the width of 5μm; (c) output field of the DEMUX when the sampling waveguide is 5μm in width; (d) the field sampled by the waveguide array with the width of 3μm; (e) output field of the DEMUX when the sampling waveguide is 3μm in width.

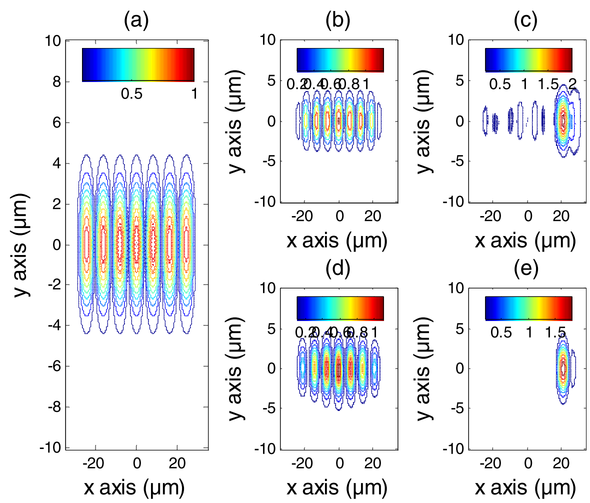

Fig. 5. The field at DEMUX input and output when the 7th mode of the rectangular core fiber is injected. (a) 7th mode of the rectangular core fiber; (b) the field sampled by the waveguide array with the width of 5μm; (c) output field of the DEMUX when the sampling waveguide is 5μm in width; (d) the field sampled by the waveguide array with the width of 3μm; (e) output field of the DEMUX when the sampling waveguide is 3μm in width.

3μm and 5μm. It should be noted that the total widths of the sampling arrays are the same while the cladding gaps are different. The corresponding sampled fields are plotted in Fig. 2 (b)–Fig. 5(b) and Fig. 2 (d)–Fig. 5(d), while the output fields of the MMI coupler are plotted in Fig. 2 (c)–Fig. 5(c) and Fig. 2 (e)–Fig. 5(e). It can be seen that the rectangular core fiber modes fulfill the sinusoidal functions. After being sampled by the waveguide array, the fields become the supermodes of the array and obey the sinusoidal law. With the increase of mode order, the output fields of the MMI coupler shift from the left to the right, clearly identifying different modes of the rectangular core fiber.

The different width of the sampling fiber will result in different performance. It can be seen from the figures that the thinner the sampling waveguide is, the better the performance of the device is. The mode extinction ratio, which is defined as the power of the corresponding output port over the power at other output ports, is investigated. The modes in the case of 3μm-wide sampling waveguide have mode extinction ratios ranging from 23 to 27dB, which are higher than those in the case of 5μm-wide sampling waveguide, especially when the mode number increases. For instance, in Fig. 2, when the input mode is the 1st mode, the mode extinction ratio is 27dB for the case of 3μm-wide sampling waveguide and 27dB for the case of 5μm-wide sampling waveguide. However, when the input mode order gets higher, e.g. mode 7 in Fig. 5, the mode extinction ratio of the device with 5μm-wide sampling waveguide degrades to 15dB while the

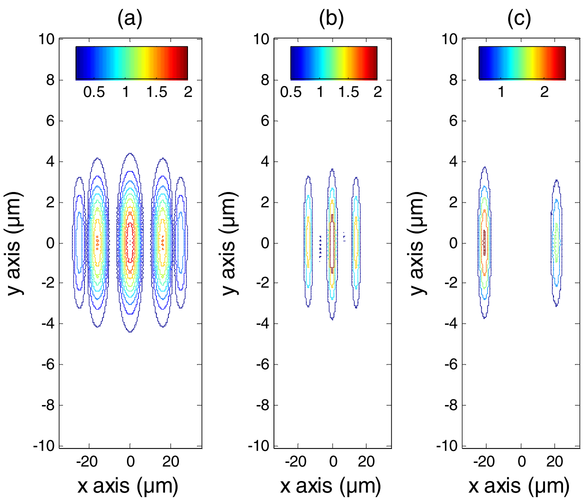

Fig. 6. De-multiplexing of the combined modal field. The ratio of mode 1 and mode 7 is 1:1. (a) The combined mode 1 and mode 7 with equal phase. (b) Sampled combined mode. (c) De-multiplexed modes at the output of the device.

other remains unchanged. Although wider sampling arrays result in lower mode extinction ratios, they can capture more output power of the fiber. For instance, for the 1st mode, the insertion loss will be 0.4dB for 5μm-wide sampling waveguide and 0.8dB for 5μm-wide sampling waveguide. Hence, the width should be carefully chosen. In our simulation, the width of 3μm seems to be an optimized choice.

To further demonstrate the de-multiplexing capability of the device, the 1st mode and the 7th mode of the fiber are combined with the same phase and the amplitude ratio of 1:1 and used as the input. The input field and the de-multiplexed field are illustrated in Fig. 6 with sampling waveguide to be 3μm wide. The two modes have been successfully separated, while the power of the higher order mode is slightly lower than that of the lower order mode. The calculation shows the insertion loss difference between the two modes is about 1.5dB for 3μm-wide sampling waveguide and 0.4dB for 5μm-wide sampling waveguide. This is in agreement with Eq. (4), which indicates a lower power capture efficiency for the higher order modes.

It should be noted that the capability of the device to distinguish the modes is limited to the modes below order N, because the number of the super-modes in the $N-1$ coupled sampling waveguides is $N-1$. If the 8th mode is injected into the above device, the sampled modal field will be zero. In order to increase the number of distinguishable modes, one should increase the number of the waveguides in the sampling array.

Finally, fabrication error analysis is conducted. The impact of the fabrication inaccuracies of the phase shifter and the MMI coupler have been analyzed in [14] and readers can refer to it for details. The impact of the wavelength variation can be proportionally related to the impact of the length variation of the MMI couplers [8]. It is found that the wavelength should be within 1550+/−35nm if the mode extinction ratio is above 23dB. There is one more source of the fabrication error, i.e. the mismatch between the sampling array and the rectangular core fiber. When the sampling waveguides and the rectangular core fiber have a misalignment of 1μm, the mode extinction ratio will degrade to 16dB. Therefore, we should not only adjust the phase and the width/length of the MMI coupler [10], but also take care of the sampling waveguide alignment with respect to the rectangular core fiber. Last but not the least, the anti-reflection coating technique should be applied to eliminate the back reflection to ensure the performance.

IV. Conclusion

In summary, a new method to realize mode DEMUXs for rectangular waveguides is proposed. With $N-1$ parallel waveguides sampling the optical field, the device is able to distinguish $N-1$ different modes. The method provides a general approach for the mode discrimination in rectangular waveguides with high mode extinction ratio.

References

[1] H. R. Stuart, "Dispersive multiplexing in multimode optical fiber," *Science*, vol. 289, pp. 281–283, Jul. 2000.

[2] S. Berdague and P. Facq, "Mode division multiplexing in optical fibers," *Appl. Opt.*, vol. 21, no. 11, pp. 1950–1955, 1982.

[3] B. C. Thomsen, "MIMO enabled 40 Gb/s transmission using mode division multiplexing in multimode fiber," in *Proc. Conf. OFC/NFOEC*, 2010, pp. 1–3.

[4] A. K. Sridharan, P. H. Pax, J. E. Heebner, D. R. Drachenberg, J. P. Armstrong, and J. W. Dawson, "Mode-converters for rectangular-core fiber amplifiers to achieve diffraction-limited power scaling," *Opt. Exp.*, vol. 20, no. 27, pp. 28792–28800, 2012.

[5] A. L. Bullington, P. H. Pax, A. K. Sridharan, J. E. Heebner, M. J. Messerly, and J. W. Dawson, "Mode conversion in rectangular-core optical fibers," *Appl. Opt.*, vol. 51, no. 1, pp. 84–88, 2012.

[6] M. Bachmann, P. A. Besse, and H. Melchior, "General self-imaging properties in N×N multimode interference couplers including phase relations," *Appl. Opt.*, vol. 33, no. 18, pp. 3905–3911, 1994.

[7] J. M. Heaton and R. M. Jenkins, "General matrix theory of self-imaging in multimode interference (MMI) couplers," *IEEE Photon. Technol. Lett.*, vol. 11, no. 2, pp. 212–214, Feb. 1999.

[8] A. R. Gupta, K. Tsutsumi, and J. Nakayama, "Synthesis of Hadamard transformers by use of multimode interference optical waveguides," *Appl. Opt.*, vol. 42, no. 15, pp. 2730–2738, 2003.

[9] S.-Y. Tseng, Y. Kim, C. J. K. Richardson, and J. Goldhar, "Implementation of discrete unitary transformations by multimode waveguide holograms," *Appl. Opt.*, vol. 45, no. 20, pp. 4864–4872, 2006.

[10] J. Leuthold, R. Hess, J. Eckner, P. A. Besse, and H. Melchior, "Spatial mode filters realized with multimode interference couplers," *Opt. Lett.*, vol. 21, no. 11, pp. 836–838, 1996.

[11] J. Leuthold, J. Eckner, E. Gamper, P. A. Besse, and H. Melchior, "Multimode interference couplers for the conversion and combining of zero- and first-order modes," *J. Lightw. Technol.*, vol. 16, no. 7, pp. 1228–1239, Jul. 1998.

[12] A. L. Y. Low, Y. S. Yong, A. H. You, S. F. Chien, and C. F. Teo, "A five-order mode converter for multimode waveguide," *IEEE Photon. Technol. Lett.*, vol. 16, no. 7, pp. 1673–1675, Jul. 2004.

[13] J. B. Park, D.-M. Yeo, and S.-Y. Shin, "Variable optical mode generator in a multimode waveguide," *IEEE Photon. Technol. Lett.*, vol. 18, no. 20, pp. 2084–2086, Oct. 15, 2006.

[14] J. Zhou and P. Gallion, "A novel mode multiplexer/demultiplexer for multi-core fibers," *IEEE Photon. Technol. Lett.*, vol. 25, no. 13, pp. 1214–1217, Jul. 1, 2013.

[15] J. Zhou and P. Gallion, "A mode MUX/DEMUX for multicore fibers with 2D core arrays," *IEEE Photon. Technol. Lett.*, vol. 26, no. 13, pp. 1336–1339, Jul. 1, 2014.

[16] E. Kapon, J. Katz, and A. Yariv, "Supermode analysis of phase-locked arrays of semiconductor lasers," *Opt. Lett.*, vol. 9, no. 4, pp. 125–127, 1984.

[17] F. Saitoh, K. Saitoh, and M. Koshiba, "A design method of a fiber-based mode multi/demultiplexer for mode-division multiplexing," *Opt. Exp.*, vol. 18, no. 5, pp. 4709–4716, 2010.

[18] X. Yang *et al.*, "Primary experiments on 2-D and 1-D fiber-type optical phased array," *Proc. SPIE*, vol. 7136, p. 71363J, Nov. 2008.